

# Resolving the Transition from Molecular to Atomic at 1/5 Solar Metallicity in the Small Magellanic Cloud

Katherine E. Jameson<sup>1</sup>, Alberto D. Bolatto<sup>1</sup>, Mark Wolfire<sup>1</sup>,  
Monica Rubio<sup>2</sup>, Rodrigo Herrera Camus<sup>1,3</sup> and the HS<sup>3</sup> Collaboration

<sup>1</sup>Astronomy Department and Laboratory for Millimeter-wave Astronomy, University of Maryland, College Park, MD, 20742, USA  
email: [kjameson@astro.umd.edu](mailto:kjameson@astro.umd.edu)

<sup>2</sup>Departamento de Astronomía, Universidad de Chile, Camino El Observatorio 1515, Casilla 36-D, Santiago, Chile

<sup>3</sup>Max-Planck-Institut für Extraterrestrische Physik, Giessenbachstrasse, D-85748 Garching, Germany

**Abstract.** At a distance of 61 kpc, the Small Magellanic Cloud (SMC) affords an absolutely unique view of the low metallicity star-forming interstellar medium, providing the nearest laboratory to study processes relevant to star formation at high redshifts. We present new ALMA 7m-array maps of <sup>12</sup>CO and <sup>13</sup>CO (2 – 1) for one of the four observed regions in the Southwest Bar of the SMC. These maps are the first high-resolution ( $\sim 6'' \sim 1.7$  pc) images of CO in a molecular cloud at 1/5 Solar metallicity. We show the structure of photodissociation regions for the first time at 1/5 Solar metallicity by combining the new ALMA data with Herschel maps of [C II] and [O I]. We present preliminary evidence that there is extended, faint <sup>12</sup>CO (2 – 1) emission near where we expect the H I-to-H<sub>2</sub> transition. We also compare our data to the low metallicity 3D simulations by Glover & Mac Low (2011) and Shetty *et al.* (2011).

**Keywords.** ISM: clouds, ISM: structure, galaxies: ISM, Magellanic Clouds

---

## 1. Introduction

Due to its proximity and our ability to achieve high spatial resolution, the SMC provides the ideal laboratory to study detailed properties of the molecular gas in star-forming regions in a low mass,  $M_{*,\text{SMC}} = 3 \times 10^8 M_{\odot}$  (Skibba *et al.* 2012), and low metallicity,  $Z_{\text{SMC}} \sim 1/5 Z_{\odot}$  (Pagel 2003), environment. In low metallicity environments <sup>12</sup>CO, the most common tracer of the total amount of molecular gas (dominated by H<sub>2</sub>), emits weakly and often goes undetected. The SMC has been studied extensively in <sup>12</sup>CO with the earliest surveys completed using the Columbia 1.2m (Rubio *et al.* 1991). The early survey of both Clouds (Israel *et al.* 1993) and of the Southwest Bar of the SMC (Rubio *et al.* 1993) using the Swedish-ESO Submillimetre Telescope (SEST) showed the CO emission to be under-luminous compared to the Milky Way by a factor of a few at small scales ( $\sim 10$  pc) and by  $\sim 10 - 20$  at large scales ( $\sim 200$  pc) in the SMC. A “CO-faint” molecular phase is predicted by analytical and numerical models that show the CO abundance drops off below a mean visual extinction of  $A_V \sim 2$  mag (Wolfire *et al.* 2010; Glover & Mac Low 2011; Shetty *et al.* 2011) where most carbon exists as C<sup>+</sup> while H<sub>2</sub> remains molecular because it is strongly self-shielding (Tielens & Hollenbach 1985; Wolfire *et al.* 1989; Kaufman *et al.* 1999). Studies of the SMC find this phase to encompass 80% – 90% of all the H<sub>2</sub> (Israel 1997; Pak *et al.* 1998; Leroy *et al.* 2007; Leroy *et al.* 2011; Bolatto *et al.* 2011), likely dominating the molecular reservoir available to star formation.

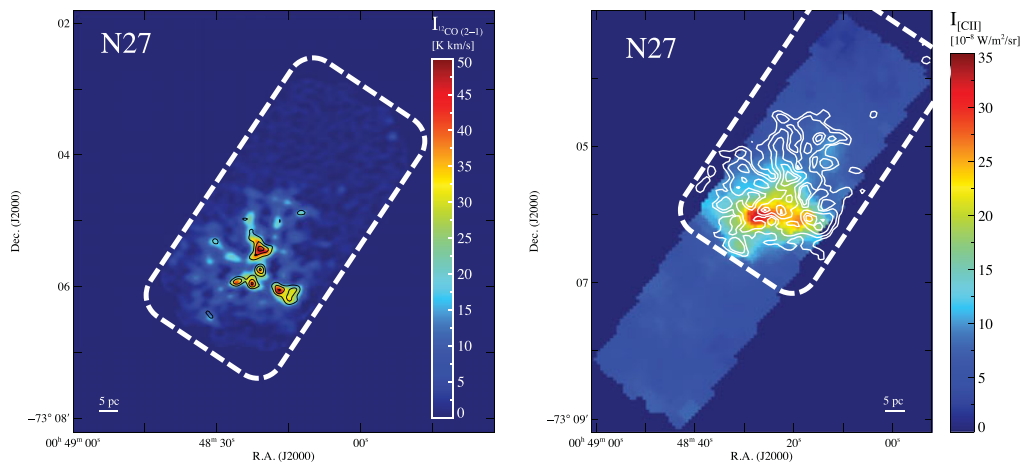


**Figure 1.** Left: Integrated intensity map of the combined ALMA 7m-array and APEX single-dish  $^{12}\text{CO}$  (2 – 1) image of the N27 region with black contours showing the  $^{13}\text{CO}$  (2 – 1) integrated intensity map at 2, 4, and 6 K km s $^{-1}$  (beam size  $\sim 7'' \times 5''$ ). In both panels the dashed white lines shows the approximate coverage of the ALMA 7-m array map. Right: Image of the [C II] integrated intensity for the N27 region with white contours showing the combined CO integrated intensity map at 3, 6, 15, 30, 40, and 50 K km s $^{-1}$ . We see evidence of faint  $^{12}\text{CO}$  emission out to low  $A_V$  and close to the expected atomic-to-molecular transition, and there is similarity between the [C II] and CO structure, which suggests that CO is tracing the molecular cloud structure.

The “CO-faint” molecular gas can be traced using diffuse  $\gamma$ -rays, dust continuum emission, and [C II] and [O I] line emission. Large-scale maps of the total molecular gas in the SMC have been made using dust continuum emission using *Spitzer* data (Leroy *et al.* 2007; Leroy *et al.* 2009; Bolatto *et al.* 2011), and more recently *Herschel* data (Jameson *et al.* 2015a), that show more extended molecular gas than what is traced by the large-scale NANTEN  $^{12}\text{CO}$  map (Mizuno *et al.* 2001). Using the dust-based molecular gas estimate, Jameson *et al.* (2015a) finds no strong evidence that low metallicity affects the large-scale relationship between star formation and molecular gas, but metallicity is expected to affect the small-scale structure of the molecular gas and their surrounding photodissociation regions. The emission from [C II] can also trace the “CO-faint” molecular phase (e.g., Madden *et al.* 1997; Pineda *et al.* 2013), and observations from *Herschel* allow us to attain high resolution ( $\sim 10''$ ) [C II] maps. When combined with new high resolution  $^{12}\text{CO}$  maps from ALMA ( $\sim 6''$  resolution), we can study the structure of the molecular gas and resolve the H I-to- $\text{H}_2$  transition. We present new *Herschel* [C II] and ALMA CO data for one of the targeted regions in the Southwest Bar of the SMC and show that there appears to be faint CO emission near the H I-to- $\text{H}_2$  transition.

## 2. Observations

Our results are based on our new ALMA 7m-array CO observations and *Herschel* [C II] and [O I] data. The *Herschel* data come from the *Herschel* Spectroscopic Survey of the SMC (HS $^3$ ; Jameson *et al.* 2015b). The survey consists of four  $1.5' \times 6'$  strips covering star-forming regions and one  $2' \times 2'$  map targeted at a peak in the dust-based molecular gas estimate not detected in the NANTEN  $^{12}\text{CO}$  map. The regions sample a range of radiation field strength, star formation, and detected molecular gas in the Southwest Bar and in N83/N84 of the SMC. We mapped four approximately  $1.5' \times 3'$

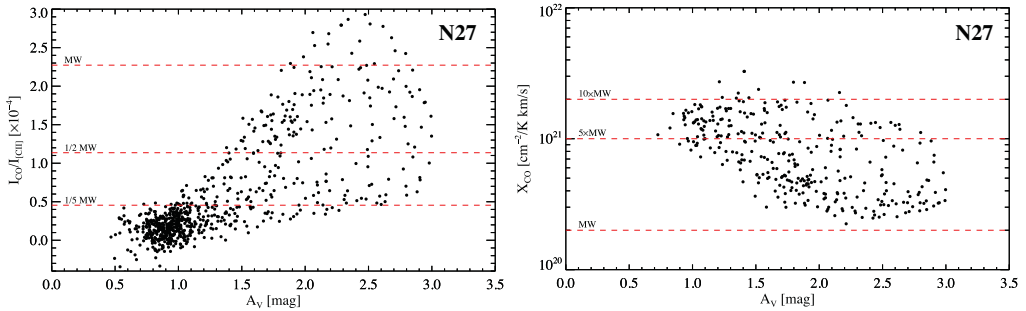


**Figure 2.** Left: The ratio of the integrated intensity of  $^{12}\text{CO}$  (using the APEX  $^{12}\text{CO}$  (2 – 1) data and assuming thermalized emission to convert to (1 – 0)) to that of [C II] as a function of  $A_V$  for the N27 region in the SMC. The red dashed lines indicate different scalings of the canonical value for the Milky Way of  $\sim 1/4400$  (Stacey *et al.* 1991). Right: The CO-to- $\text{H}_2$  conversion factor ( $X_{\text{CO}}$ ) using [C II]-based estimate of  $N_{\text{H}_2}$  (assuming all [C II] emission comes from molecular gas) with  $\geq 3\sigma$   $^{12}\text{CO}$  (2 – 1) detections for the N27 region. The red dashed lines show different scalings of  $X_{\text{CO}}$  for the Milky Way of  $2 \times 10^{20} \text{ cm}^{-2} (\text{K km s}^{-1})^{-1}$  (Bolatto *et al.* 2013).

regions overlapping the HS<sup>3</sup> regions in  $^{12}\text{CO}$ ,  $^{13}\text{CO}$ , and  $\text{C}^{18}\text{O}$  (2 – 1) in the Southwest Bar with the ALMA 7m-array (resolution  $\sim 6''$ ). The ALMA 7m-array maps have been combined with single-dish data from APEX ( $\theta = 29.5''$ ; Rubio *et al.* 2015). For the preliminary results, we focus on the N27 region.

### 3. Preliminary Results

The [C II] and [O I] lines were detected ( $S/N \gtrsim 3$ ) throughout all of the HS<sup>3</sup> regions. The ALMA 7m-array data shows clear detections of  $^{12}\text{CO}$  and  $^{13}\text{CO}$  (2 – 1) emission in all of the regions, but  $\text{C}^{18}\text{O}$  is not detected (see Figure 1). In N27, we find  $^{12}\text{CO}/^{13}\text{CO}$  ratios of  $\sim 10 - 15$  in the peaks of the  $^{12}\text{CO}$  map, which is consistent with previous measurements (Israel *et al.* 2003) and the typical ratios observed in the Milky Way. We see good correspondence between the  $^{12}\text{CO}$  and [C II] emission and a fairly flat [O I]/[C II] ratio of  $\sim 0.3$  across the regions. We investigate the structure of the photodissociation region and molecular cloud by using the visual extinction ( $A_V$ ) as an indicator of depth within the cloud. The optical depth at  $160 \mu\text{m}$  ( $\tau_{160}$ ) map from Lee *et al.* (2015) is converted to  $A_V$  using  $A_V \sim 2200\tau_{160}$ . The left panel of Figure 2 shows that the CO/[C II] ratio in N27 tends to increase at higher  $A_V$  deeper into the cloud and reach ratios similar to the value found in the Milky Way. Finding CO/[C II] and  $^{12}\text{CO}/^{13}\text{CO}$  ratios similar to the Milky Way is consistent with theoretical expectations that once enough dust shielding is built up, the structure at low metallicity will resemble that of a high metallicity cloud.

An  $A_V \sim 1$  corresponds to the typical extinction where  $^{12}\text{CO}$  becomes optically thick. Our observation of faint  $^{12}\text{CO}$  emission at  $A_V < 1$  indicates that we are tracing optically thin  $^{12}\text{CO}$  emission that corresponds to the “CO-faint” molecular gas (Wolfire *et al.* 2010). Figure 2 shows [C II] emission from the cloud depths we would expect to see a significant amount of “CO-faint” molecular gas and we have some detections of  $^{12}\text{CO}$  (2 – 1) down to an  $A_V \sim 0.5$ , which is close to the expected range for the H I-to- $\text{H}_2$  ( $A_V \sim 0.2 - 0.4$ ). This suggests that this translucent molecular phase is “CO-faint” as opposed to the terminology that refers to it as “CO-dark” gas. The lower CO/[C II] ratios relative to the Milky Way value is likely indicating the presence of this “CO-faint” component where the carbon primarily exists as  $\text{C}^+$  and not as CO.

The extended, low level [C II] emission can potentially emanate from ionized gas, warm neutral medium (WNM), cold neutral medium (CNM), a translucent molecular phase, or some combination. The HS<sup>3</sup> data includes [N II] observations, but there are no detections in the SMC regions, which indicates that the ionized gas is not contributing to the [C II] emission. The [O I]/[C II] ratio is a good indicator of the density of the gas, and comparing the ratio values to new heating and cooling curves for the SMC from Wolfire *et al.* (2015) show that the values we observe indicate densities of  $n \sim 100 - 300 \text{ cm}^{-3}$ . These densities correspond to the CNM and potentially molecular gas. Combined with the observation that the extended [C II] and <sup>12</sup>CO emission structure is similar to that seen for the mid-IR H<sub>2</sub> rotational lines, it is likely that this gas contains a molecular component.

We then make the simplifying assumption that all of the [C II] emission originates from H<sub>2</sub> gas, and convert the observed [C II] intensity into an H<sub>2</sub> column density ( $N_{\text{H}_2}$ ) using the [C II] cooling curve for the SMC from Wolfire *et al.* (2015). This produces [C II]-based estimates of  $N_{\text{H}_2} \sim 1 - 2 \times 10^{21} \text{ cm}^{-2}$ . Using these values of  $N_{\text{H}_2}$ , we estimate the <sup>12</sup>CO-to-H<sub>2</sub> conversion factor  $X_{\text{CO}}$  (see Figure 2, right panel). The general trend of decreasing  $X_{\text{CO}}$  with increasing  $A_V$  is consistent with the results for a LMC/SMC-type molecular cloud from Shetty *et al.* (2011) and can be explained by the enhanced photodissociation of CO in the outskirts of the cloud at lower metallicity.

## References

- Bolatto, A. D., Leroy, A. K., Jameson, K., *et al.* 2011, *ApJ*, 741, 12  
 Bolatto, A. D., Wolfire, M., & Leroy, A. K. 2013, *ARA&A*, 51, 207  
 Glover, S. C. O. & Mac Low, M.-M. 2011, *MNRAS*, 412, 337  
 Israel, F. P., Johansson, L. E. B., Lequeux, J., *et al.* 1993, *A&A*, 276, 25  
 Israel, F. P. 1997, *A&A*, 328, 471  
 Israel, F. P., Johansson, L. E. B., Rubio, M., *et al.* 2003, *A&A*, 406, 817  
 Jameson, K. E., Bolatto, A. D., Leroy, A. K., *et al.* 2015, *ApJ*, submitted (arXiv:1510.08084)  
 Jameson, K. E., Bolatto, A. D., Wolfire, M., *et al.* 2015, *in prep*  
 Kaufman, M. J., Wolfire, M. G., Hollenbach, D. J., & Luhman, M. L. 1999, *ApJ*, 527, 795  
 Lee, C., Leroy, A. K., Schnee, S., *et al.* 2015, *MNRAS*, 450, 2708  
 Leroy, A., Bolatto, A., Stanimirović, S., *et al.* 2007, *ApJ*, 658, 1027  
 Leroy, A. K., Bolatto, A., Bot, C., *et al.* 2009, *ApJ*, 702, 352  
 Leroy, A. K., Bolatto, A., Gordon, K., *et al.* 2011, *ApJ*, 737, 12  
 Madden, S. C., Poglitsch, A., Geis, N., Stacey, G. J., & Townes, C. H. 1997, *ApJ*, 483, 200  
 Mizuno, N., Yamaguchi, R., Mizuno, A., *et al.* 2001, *PASJ*, 53, 971  
 Pagel, B. E. J. 2003, in: Charbonnel, C. and Schaerer, D. and Meynet, G. (eds.), *CNO in the Universe*, ASP Conference Series Volume 304 (San Francisco: ASP), p. 187  
 Pak, S., Jaffe, D. T., van Dishoeck, E. F., Johansson, L. E. B., *et al.* 1998, *ApJ*, 498, 735  
 Pineda, J. L., Langer, W. D., Velusamy, T., & Goldsmith, P. F. 2013, *A&A*, 554, A103  
 Rubio, M., Garay, G., Montani, J., & Thaddeus, P. 1991, *ApJ*, 368, 173  
 Rubio, M., Garay, G., Montani, J., & Thaddeus, P. 1991, *ApJ*, 368, 173  
 Rubio, M., Lequeux, J., & Boulanger, F. 1993, *A&A*, 271, 9  
 Rubio, M., Bolatto, A. D., Jameson, K. E., *et al.* 2015, *in prep*  
 Shetty, R., Glover, S. C., Dullemond, C. P., *et al.* 2011, *MNRAS* 415, 3253  
 Skibba, R. A., Engelbracht, C. W., Aniano, G., *et al.* 2012, *ApJ* 761, 42  
 Stacey, G. J., Geis, N., Genzel, R., *et al.* 1991, *ApJ*, 373, 423  
 Tielens, A. G. G. M. & Hollenbach, D. 1985, *ApJ*, 291, 722  
 Wolfire, M. G., Hollenbach, D., & Tielens, A. G. G. M. 1989, *ApJ* 344, 770  
 Wolfire, M. G., Hollenbach, D., & McKee, C. F. 2010, *ApJ* 716, 1191  
 Wolfire, M. G., *et al.* 2015, *in prep*